



ELSEVIER

Earth and Planetary Science Letters 202 (2002) 275–288

EPSL

www.elsevier.com/locate/epsl

Preliminary analysis of the Knipovich Ridge segmentation: influence of focused magmatism and ridge obliquity on an ultraslow spreading system

Kyoko Okino^{a,*}, Daniel Curewitz^a, Miho Asada^a, Kensaku Tamaki^a, Peter Vogt^b, Kathleen Crane^c

^a *Ocean Research Institute, University of Tokyo, 1-15-1 Minamidai, Nakano, Tokyo 164-8639, Japan*

^b *Naval Research Laboratory, Washington, DC 20375, USA*

^c *NOAA, Silver Spring, MD 20910, USA*

Received 28 January 2002; received in revised form 7 June 2002; accepted 19 June 2002

Abstract

Bathymetry, gravity and deep-tow sonar image data are used to define the segmentation of a 400 km long portion of the ultraslow-spreading Knipovich Ridge in the Norwegian–Greenland Sea, Northeast Atlantic Ocean. Discrete volcanic centers marked by large volcanic constructions and accompanying short wavelength mantle Bouguer anomaly (MBA) lows generally resemble those of the Gakkel Ridge and the easternmost Southwest Indian Ridge. These magmatically robust segment centers are regularly spaced about 85–100 km apart along the ridge, and are characterized by accumulated hummocky terrain, high relief, off-axis seamount chains and significant MBA lows. We suggest that these eruptive centers correspond to areas of enhanced magma flux, and that their spacing reflects the geometry of underlying mantle upwelling cells. The large-scale thermal structure of the mantle primarily controls discrete and focused magmatism, and the relatively wide spacing of these segments may reflect cool mantle beneath the ridge. Segment centers along the southern Knipovich Ridge are characterized by lower relief and smaller MBA anomalies than along the northern section of the ridge. This suggests that ridge obliquity is a secondary control on ridge construction on the Knipovich Ridge, as the obliquity changes from 35° to 49° from north to south, respectively, while spreading rate and axial depth remain approximately constant. The increased obliquity may contribute to decreased effective spreading rates, lower upwelling magma velocity and melt formation, and limited horizontal dike propagation near the surface. We also identify small, magmatically weaker segments with low relief, little or no MBA anomaly, and no off-axis expression. We suggest that these segments are either fed by lateral melt migration from adjacent magmatically stronger segments or represent smaller, discrete mantle upwelling centers with short-lived melt supply. © 2002 Elsevier Science B.V. All rights reserved.

Keywords: mid-ocean ridges; segmentation; sea-floor spreading; gravity anomalies; sonar methods; Arctic Region

* Corresponding author. Tel.: +81-3-5351-6446; Fax: +81-3-5351-6445.

E-mail address: okino@ori.u-tokyo.ac.jp (K. Okino).

1. Introduction

What thermo-mechanical processes control the observed large morphological, geological, and geophysical variation between ridges? This is a fundamental question facing modern investigation of mid-ocean ridge tectonics and geophysics [1]. Although spreading rate appears to be a main parameter influencing these processes, another important factor is the interplay between spreading rate and magma supply, reflecting the physical characteristics of the lithosphere and asthenosphere. Fast and slow spreading systems represented by the East-Pacific Rise (EPR) and the Mid-Atlantic Ridge (MAR), respectively, have been extensively studied over the last two decades. However, the slowest end-members of the world's ridge system, ultraslow spreading centers with full spreading rates less than 20 mm/yr, have recently been targeted for systematic analysis. Previous global ridge comparisons and analyses have shown that crustal thicknesses are almost constant (7 km) from the fast spreading EPR (150 mm/yr) to the slow spreading MAR (20 mm/yr) [2–4]. In contrast, anomalously thin crust is observed at ultraslow spreading centers using seismic refraction [5] and gravity analyses [6]. Therefore ultraslow spreading systems provide unique natural laboratories to investigate fundamental problems of oceanic crustal accretion. Two well-known ultraslow spreading systems in the world, the Arctic Ridges [7–9] and the Southwest Indian Ridge (SWIR) [10–12] have long remained unsurveyed primarily because of their remote geographical locations.

The Arctic Ridges extend north of the Mid-Atlantic Ridge system, and consist of the Kolbeinsey, Mohns, Knipovich and Gakkel ridges. Recent sub-ice studies on the Gakkel Ridge reveal that the ridge (full spreading rate < 10 mm/yr in its eastern half) is not offset by transform faults for over 1000 km [9], the oceanic crust is extremely thin [6], and mantle rocks are exposed along the ridge axis [13]. The Knipovich Ridge is located between 73°45'N and 78°35'N, between Greenland and Svalbard (Fig. 1). This is the northernmost portion of the Arctic Ridges free from the Arctic Ocean ice canopy and readily

accessible to surface vessels. The Knipovich Ridge is transform-free along its entire length, and is characterized by high obliquity ($\phi = 35\text{--}50^\circ$, where ϕ is the angle between the spreading direction and the normal to the ridge trend) [14] and a heavily sedimented rift axis due to its location close to the Eurasian continental margin [15]. During an interdisciplinary cruise on the Knipovich Ridge in September 2000 (K2K cruise, [16]) using the *R/V Professor Logachev* (VNIIO, St. Petersburg, Russia), we acquired along-axis deep-tow side scan sonar images and collected water geochemistry data for evidence of hydrothermal activity. Detailed analyses of these two datasets are the subject of other papers. In this paper we combine previously collected datasets (bathymetry and satellite derived gravity), a new along-axis bathymetric profile, and sonar images to define the segmentation of this ultraslow, oblique spreading system. Our discussion focuses on the segmentation pattern and its implications for crustal accretion under ultraslow and variably oblique spreading conditions. We compare the spacing and amplitude of discrete, focused magma upwelling centers on the Knipovich Ridge to results from other ultraslow spreading systems with varying degrees of obliquity.

2. Tectonic background

The Arctic Mid-ocean Ridge system extends northward from the MAR and is the boundary between the Eurasian and North American Plates. The pole of relative motion between these plates is located in Siberia [17], so the full spreading rate decreases northward from 18 mm/yr on the Kolbeinsey Ridge to less than 10 mm/yr on the eastern Gakkel Ridge. The Arctic Ridge system began opening at Chron 24 [7], about 53 Ma on the Cande and Kent [18] time scale, splitting the Lomonosov Ridge and Greenland from the Eurasian continent. Aeromagnetic data show continuous spreading along the Gakkel Ridge since Chron 24, with some variation in spreading rate [7]. The data also reveal the spreading history of the Mohns Ridge, where the spreading direction changed from NNW–SSE to NW–SE at Chron

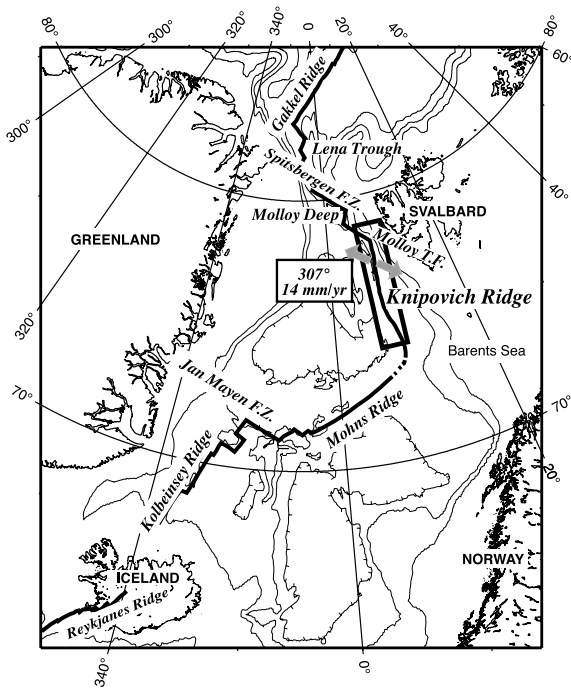


Fig. 1. Tectonic setting of the Norwegian–Greenland Sea and location of the study area (box) along the Knipovich Ridge. Thick lines show the present plate boundary and gray arrows indicate the current plate motion direction [17]. Bathymetric contour interval is 1000 m.

7 [19,20] (about 25 Ma [18]). The history of the Knipovich Ridge is rather enigmatic, because neither the aeromagnetic data nor the limited ship-track data show clear magnetic anomaly patterns. The Knipovich Ridge has been suggested to have originated as a shear-zone or continental transform that linked the Gakkal and Mohns ridges during the early history of the Arctic Ridge system (e.g., [20]). This transform became a spreading center either through linkage of an echelon sub-basins or through ridge propagation from the Mohns Ridge following the change of plate motion at Chron 7. An asymmetric spreading history [21] and a ridge jump at Eocene time [22] have also been proposed; however, the detailed history of the Knipovich Ridge is still under discussion.

The Knipovich Ridge is now an ~ 550 km long, transform-free ridge segment linking the Molloy transform fault at its northern end and the Mohns Ridge at its southern end (Fig. 1).

Present global plate motion models predict 307° spreading at $15\text{--}17$ mm/yr at the Knipovich Ridge. The general trend of the rift wall is 002° north of $75^\circ 50'N$ and 347° south of that point, resulting in variably oblique spreading along the entire ridge. The obliquity, the angle between the normal to the axial rift valley and the plate motion vector, is 35° in the north and 49° in the south. The surface structure of the Knipovich Ridge, therefore, is formed by the combined effect of tectonism and volcanism under oblique spreading conditions [23].

3. Data analyses

3.1. Data sources

No multibeam bathymetry data have been collected along the Knipovich Ridge, so we compiled the bathymetry from three different data sources. The IBCAO digital database [24], a compilation of ship-track data in the Arctic and Northeast Atlantic oceans (north of $70^\circ N$), contains 1.5 km gridded depths over the Knipovich Ridge. The original track lines are sparse in our study area, so short wavelength features are not recorded. The northern half of the Knipovich Ridge was surveyed using SeaMARCII sonar in 1989 and 1990 by Crane et al. [25]. The detailed bathymetry synthesized from SeaMARCII phase return data is available within 40–50 km off-axis for the regions north of $75^\circ 50'N$, where depth values are spaced at < 100 m intervals along and across track. Obvious artifacts along the sonar track are present in the dataset; however, their amplitude is not large enough to cause serious problems for gravity analysis. The third dataset we used is the along-axis 3.5 kHz depths collected during the K2K cruise. These data encompass a 400 km long profile of the axial valley, $\sim 75\%$ of the length of the ridge along a single ship's track. Comparison of the three datasets along the northern Knipovich Ridge (Fig. 2) shows good agreement between 3.5 kHz and SeaMARCII phase data, and shows that the IBCAO dataset misses short wavelength features. We combined these three datasets to make a $2.5'$ by $0.625'$ (about 1150 m) grid,

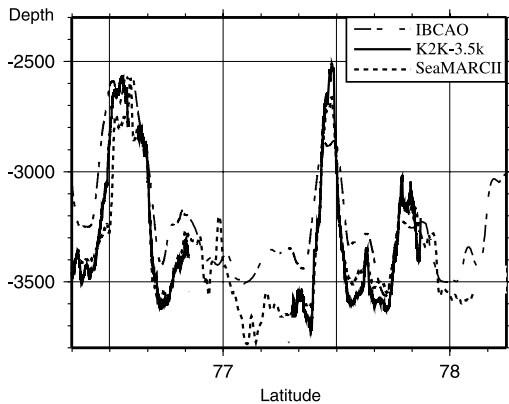


Fig. 2. Axial bathymetry profiles for the northern Knipovich Ridge (76°20'N–78°15'N) from the IBCAO-beta dataset [24], SeaMARCII sidescan sonar phase bathymetry [25] and 3.5 Hz profiler data collected during the K2K cruise [16].

using the following order of priority: 3.5 kHz, SeaMARCII, and IBCAO (Fig. 3a). We also prepared a finer grid for regions north of 76°N to examine the detailed on- and off-axis bathymetry of the ridge.

We extracted the free-air gravity anomaly (FAA) field from the 3.75' gridded database calculated from ERS-1 altimetry (Fig. 3b, [26]). The ERS-1 gravity field covers the ocean south of 81.5°N and recovers signals down to a wavelength of ~ 15 km [27].

Sediment thickness data were extracted from an isopach map compiled in a previous study [28]. The original map is expressed in two-way travel time contours at intervals of 0.5 s; these contours were digitized and transformed to thickness assuming a sediment velocity of 2.2 km/s. Sediment thicknesses are maximum (greater than 1.5 s, $\sim > 3.3$ km) near the Svalbard margin and less than 0.5 s (< 1.1 km) on the ridge axis. These data are useful for removing the large-scale influence of sedimentary layer on the MBA analysis; however, their horizontal resolution is not high enough to correct for short wavelength variations in sediment thickness.

3.2. Data analysis

The FAA (Fig. 3b) contains signals from bathymetry, sediments, and crust and mantle density

anomalies. To reveal the crust and mantle anomalies we subtracted from the FAA the theoretical gravity effects of the water–sediment, sediment–crust, and crust–mantle interfaces assuming a constant density 6 km thick model crust. The densities for water, sediment, crust, and mantle were assumed to be 1030, 2300, 2800 and 3300 kg/m³, respectively. We also calculated the effects of different sediment density values; differences among these models are negligible in considering the characteristics of the along-axis anomaly relief. Our modeling indicates that higher-resolution sediment isopach data would enhance Δ MBA calculations; however, the differences are estimated at about 5 mGal. Additionally, since increased sediment thickness in the deeper along-axis sections will act to increase Δ MBA, our calculations reflect minimum values. The resulting MBA map is shown in Fig. 3c. We did not calculate the thermal effect on gravity anomalies [29,30] because of poor off-axis age determination.

4. Results

4.1. Overview of bathymetry and gravity

The trend of the Knipovich Ridge changes at 75°50'N, from 343–350° to the south to 000–007° to the north (Fig. 3a). The trend of the rift valley is oblique to the direction predicted from the global plate motion model (307° at 76°N, [17]) and the obliquity is larger in the southern part of the ridge. Bathymetric lineaments and volcanic ridges within the rift valley trend roughly 010°–035°, nearly perpendicular to the current plate motion direction (Fig. 3a). The average depth and width of the rift valley are 3500 m and 14 km. A large seamount (relief ~ 1500 m), Logachev Seamount, is located within the rift at 76°35'N, and consists of volcanic edifices and NNE–SSW trending ridges. The second largest bathymetric high at 77°29'N also exhibits 035° trending volcanic mounds and structural lineaments. Both axial volcanic peaks anchor symmetric off-axis seamount chains that are aligned parallel to the relative plate motion direction. Bathymetric highs in the southern part of the

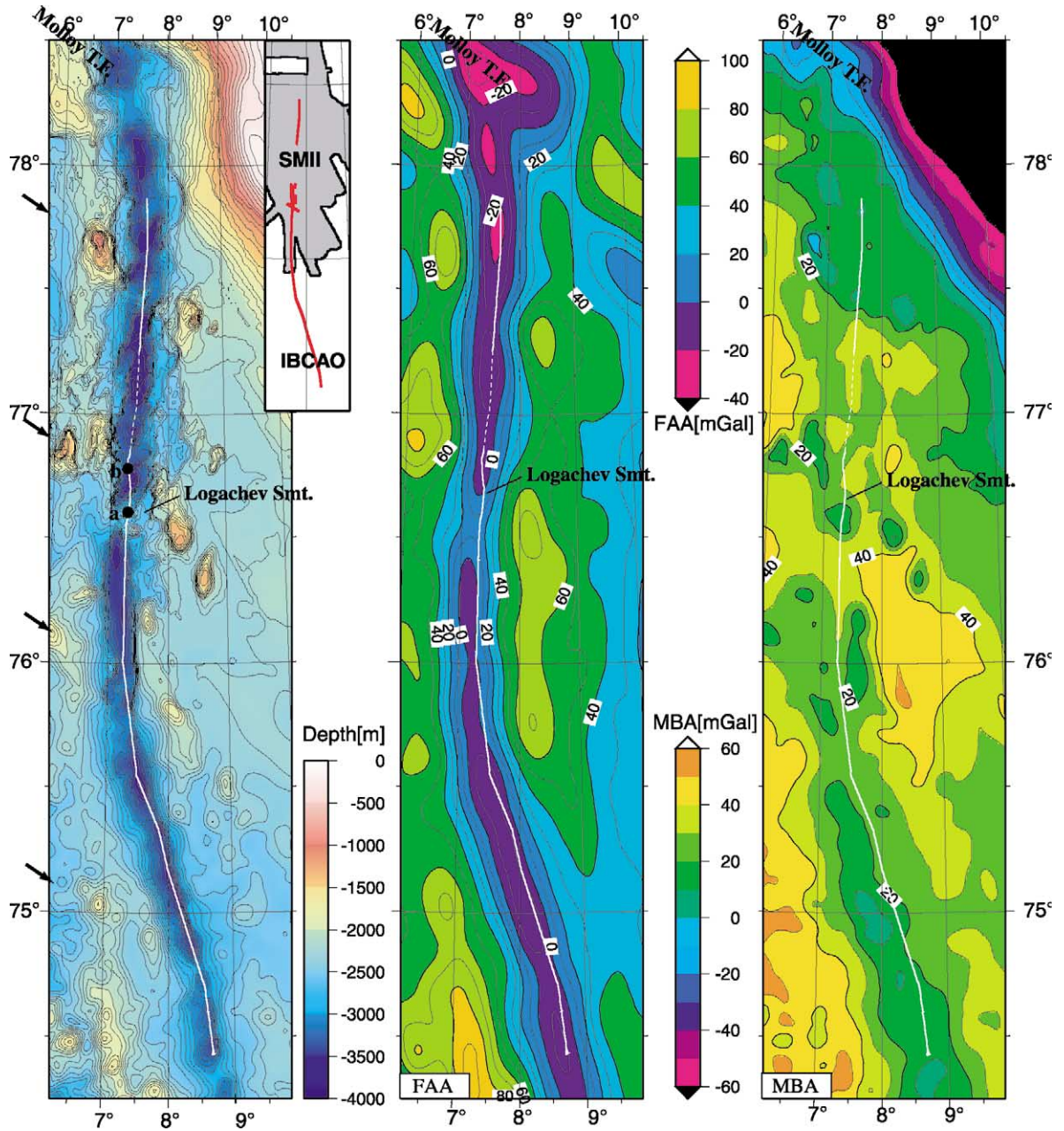


Fig. 3. (a) Color-fill bathymetric map of the Knipovich Ridge based on data from [16,24,25]. Contour interval is 100 m. White line shows the along-axis line used for bathymetry and gravity profiles in Fig. 4, which links the sonar track (solid line) and the shallowest and deepest points where the sonar track is absent (dashed line). Arrows indicate the locations of the off-axis seamount chains extending parallel to the plate motion direction. Solid black circles indicate the locations of sonar images shown in Fig. 4. Inset map shows the data sources used for compilation and red lines indicate all sonar tracks. The ship tracks used for the IBCAO program are shown in <http://www.ngdc.noaa.gov/mgg/bathymetry/arctic/IBCAOTechnicalReference.PDF>. (b) Color-fill FAA map based on satellite derived gravity [26]. Contour interval is 10 mGal. (c) Calculated MBA with 10 mGal contours.

ridge are smaller than the northern two peaks. Off-axis traces of these axial highs are also recognized in the southern part of the ridge in spite of lower depth resolution (arrows in Fig. 3a). It is likely that unmapped topographic highs exist within the southern rift valley; however, based on previous sidescan-derived phase bathymetry data (figures 12 and 13 in [25]), these highs (if present) are likely not at the same scale as the ones associated with off-axis seamount traces.

The largest negative FAA value occurs at the northern end of the ridge where the Molloy Transform Fault intersects the rift wall (Fig. 3b). Although a negative FAA trough extends along the rift, the FAA pattern is asymmetric around the rift, indicating the effect of thicker sediment to the east. After correction for sediment/crust/mantle density contrasts, the MBA (Fig. 3c) has a significant gradient on the Svalbard margin, reflecting the ocean–continent transition. The MBA map shows a few near-circular lows corresponding to on-axis bathymetric highs in the northern Knipovich Ridge and off-axis seamounts. In the southern part of the ridge, the MBA lows are centered beneath the western rift wall. This is likely due to misregistration of bathymetry in the southern area where IBCAO depths are based on a sparse and poorly navigated dataset.

4.2. Along-axis bathymetry and gravity variations

The segmentation pattern of mid-ocean ridges reflects magmatism, crustal and lithospheric structure, and mantle thermal structure. Both long and short wavelength along-axis variations in axial depth (mean = 3500 m) and MBA provide important information about ridge segmentation. Along-axis bathymetry, defined by linking centers of apparent recent volcanism with the deepest portions of the rift valley in Fig. 3a, and the MBA profile in the surveyed area display no significant long wavelength variations (Fig. 4). This suggests no large-scale variations of density and/or thermal structure along the Knipovich Ridge.

Short wavelength axial depth variations permit definition of 14 segments numbered from north to south (Fig. 4). We defined the segmentation pattern in a provisional sense, recognizing the spatial

and resolution limitations of our dataset. First we use the along-axis profile, and a positive depth variation of 100 m over 20 km along strike is used as our criterion to number the centers of the axial segments. Then we investigated our deep-towed sonar images, published sonar image and bathymetry maps [25] and gravity anomalies in identifying the segmentation. A plan view of the ridge shows segments 1–8 and the intervening deep, narrow basins corresponding to oblique non-transform discontinuities (Fig. 5). These are analogous to non-transform discontinuities along the SWIR [10] or transfer zones along the Mohns Ridge [31,32]. Volcanic constructions and fault scarps within the rift are aligned approximately perpendicular to the relative plate motion and deep sub-basins tend to elongate NW–SE. Because of data limitations and low resolution, we may have missed a segment near the boundary of the Molloy Transform Fault, and small segment centers south of 75°30'N.

The bathymetric profile is characterized by few highs and dominated by relatively long flat, deep, heavily sedimented troughs. High relief segments ($\Delta R = 963$ m and 957 m at segments 7 and 3) are only found along the northern ridge, and are associated with relatively large MBA lows ($\Delta MBA = 20$ mGal and 19 mGal, respectively). Other segments with $\Delta R = \sim 500$ m correspond to weak MBA lows ($\Delta MBA < 10$ mGal) or subtle perturbations of the MBA profile, except for segment 1 ($\Delta R = 612$ m, $\Delta MBA = 10$ mGal). The relief is lower south of 75°50'N, where the trend of the rift valley changes. The maximum relief is only 500 m, and deep, smooth seafloor dominates the southern section of the ridge. It should be noted that the track line for the along-axis profile in the southern section of the ridge was chosen using the available (low-resolution) IBCAO bathymetry data and the single track from the 1989–1990 SeaMARCII survey. The survey as it was carried out may have bypassed the summits of axial highs in the southern region for that reason. However, both our 2.5 km swath sonar image and the previous single SeaMARCII [25] swath show neither significant bathymetric peaks nor vigorous volcanic construction along long stretches of the southern axial region. The along-

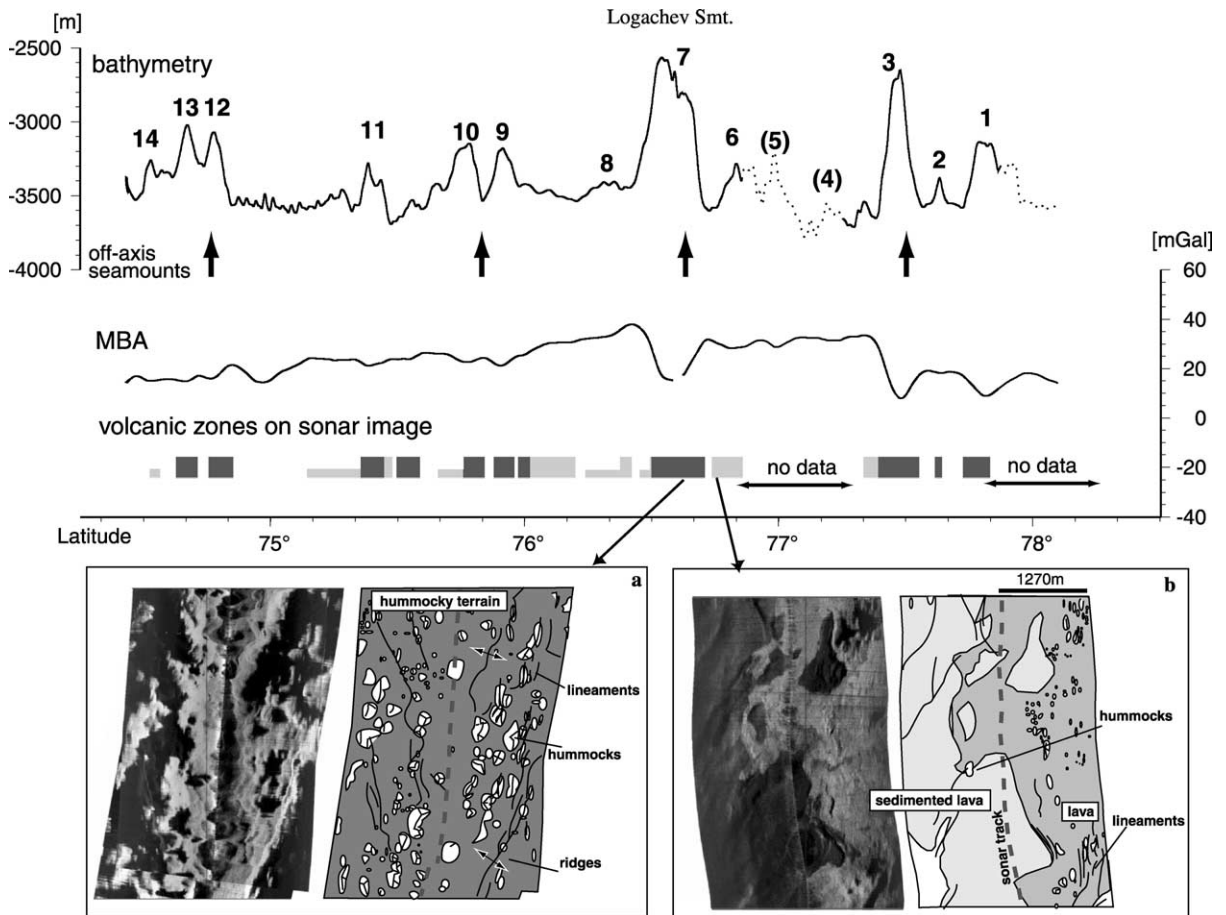


Fig. 4. Bathymetry and MBA profiles along the axis of the Knipovich Ridge between $74^{\circ}25'N$ and $78^{\circ}10'N$. Dotted bathymetry segments are not covered by deep-tow sonar images. Each ridge segment center is numbered from north to south. Arrows indicate where off-axis seamount chains meet the rift valley. Gray and dark gray blocks below the profiles indicate smooth lava flows and hummocky terrain, respectively. The height of the gray blocks corresponds to the brightness of the sonar image (tall block indicates highly reflective lava flows, probably with thin or no sediment). The blank area indicates low reflectivity seafloor. Two examples of seafloor images obtained by deep-tow sonar and their geological interpretations are shown at the bottom. (a) Hummocky terrain at $76^{\circ}38'N$; (b) smooth lava flow at $76^{\circ}48'N$ (see Figs. 3a and 5 for location).

axis profile (Fig. 4) is plotted along the general trend of the rift valley, rather than perpendicular to relative plate motion as in along-axis studies of the Mid-Atlantic Ridge [30,33] or SWIR [34,35]. This along-axis plot links the shallowest and deepest portions of the rift valley; therefore, the total relief of each segment does not vary from that obtained in other studies. However, segment lengths and the gradient of short wavelength variations may change, and require careful treatment when comparing these parameters to other ridges. Discrepancies may also arise from the lack of

high-resolution bathymetric data along the Knipovich Ridge.

4.3. Seafloor characterization using sonar images

Side-scan sonar images were collected during the K2K cruise in 2000 [16] using a deep-tow ORETEC 30 kHz sonar towed 150 m above the seafloor. Our data cover the axial zone of the Knipovich Ridge from $74^{\circ}25'N$ to $77^{\circ}50'N$ with single 2.5 km swath (Fig. 3a). The final horizontal resolution of the data ranges from 5 to 15 m. The

images were interpreted by delineating the boundaries between terrains with different acoustic textures and then investigating the distribution of volcanic and tectonic features. This information about volcanic and tectonic processes complements the bathymetry and MBA profiles. Detailed geological interpretations are the subject of a separate paper. In the present study, only the major classes of volcanic construction, hummocky mounds and smooth sheets, are considered, and we compare their distribution to along-axis bathymetry and gravity data (Fig. 4).

Hummocky mounds, amalgamations of ovoid, rough-textured lava pillows and volcanic extrusive products, are found along the entire ridge axis, but are unevenly distributed. Near the Logachev Seamount (segment 7), a large number of hummocks coalesce and form a large volcanic construction (Fig. 4a). These highly reflective hummocks are concentrated atop most bathymetric highs (segments 1–3, 7, 9–13), indicating recent focused volcanic activity, probably in the form of dike-fed eruptions [36]. Hummocks tend to align in chains that trend perpendicular to relative plate motion, possibly reflecting dike intrusion controlled by extension between the two plates. We also recognize low-reflectance hummocky textures, interpreted as older volcanic products now covered by sediment. Since the Knipovich Ridge is a sedimented ridge close to a continental margin, the hummocks and other volcanic constructions may be buried relatively soon after formation.

Smooth sheets comprise regions of high reflectivity with flat and monotonic texture. They are lobate or amorphous, and subtle wrinkles are sometimes observed on their surfaces. We interpret these as sheet-like lava flows, and, although potential source vents cannot always be identified, they are commonly found surrounding hummocky mounds and/or crater-topped cones. Additionally, these features commonly abut and cover steep scarps, indicating flow into pre-existing fault-bounded depressions (Fig. 4b). These features are most commonly observed at the base of small bathymetric highs; however, they are also found on the relatively flat area between bathymetric highs in the southern part of the ridge.

5. Discussion

5.1. Segmentation characteristics of the Knipovich Ridge

Sonar image analysis shows that segment centers either are covered by or consist of accumulated hummocks, and that most smooth lava flows are found at the base of seamounts. These observations support the interpretation that segment centers defined by the along-axis profile are the loci of recent volcanic activity. Previous investigations using long-range side-scan sonar images [25] proposed segmentation of the Knipovich Ridge into long extensional basins bounded by narrow volcanically active highs, and that the deep basins were segment centers. In this paper, we use MBA patterns and bathymetry data to propose a segmentation scheme according to models used in other slow and ultraslow spreading ridges [33,34] where elevated and magmatically active segment centers mark loci of mantle upwelling. Mid-ocean ridge segmentation patterns have been interpreted based on a variety of bathymetric, volcano-magmatic, and structural criteria [25,30,37–39] and the growing consensus is that the fundamental control on ridge segmentation is the geometry and dynamics of mantle upwelling beneath the ridge axis [40].

Although the amplitude of MBA variation is not large, the centers of segments 1, 3 and 7 correspond to prominent MBA lows (Fig. 4), indicating thicker crust and/or hotter/less dense mantle (i.e. upwelling) beneath these segment centers. Segments 3 and 7 are characterized by high relief MBA lows and off-axis seamount traces, indicating these two segments are both magmatically robust and persistent over time. Two off-axis seamount chains also intersect the axial rift near segments 9 and 10, and 12 and 13, respectively. These adjacent segments are closely spaced and they may be fed by the same mantle upwelling cell at the base of the crust. Therefore we consider each pair (segment 9/10 and segment 12/13) to be magmatically stronger and long-lived, resembling segments 3 and 7. These segments are considered to be loci of temporally stable enhanced magma fluxes, although the MBA shows little variation in

the southern Knipovich Ridge. A misfit between the location of the seafloor extrusion at segment 12/13 and the negative peak of MBA south of 75°N (Fig. 4) may indicate three-dimensional melt transport within crust, though we cannot completely exclude the effect of misregistration of bathymetry. Other segments are characterized by low relief accompanied by hummocks or lava flows indicating recent volcanism and slight or no gravity signature. We suggest that such segments are magmatically weaker: volcanism is sporadic and short-lived.

5.2. Nature of magmatically stronger segments

The Knipovich Ridge has an unusual segmentation pattern comprised of a few very high relief segments separated by long stretches of deep low relief axial valley, similar to the SWIR east of the Melville fracture zone [10]. The formation of large volcanic edifices in an axial rift requires some combination of isostatic and dynamic support of these volcanic peaks. In the previous analysis and modeling [34,39,41] a predomination of direct, rapid transport of magma from the mantle to the surface rather than storage in mid-crustal magma chambers is required to construct these edifices. Rapid magma transport to the surface through dikes is also required, with little en route crystallization and low melt supply [34]. Magmatically stronger segments of the Knipovich Ridge may correspond to mantle upwelling cells within relatively cold mantle beneath this ultraslow spreading system, where magma transport through dikes directly from mantle source to surface plays an important role in constructing large volcanic mountains within the rift valley. Magmatically weaker segments may reflect melt migration from adjacent stronger segments [42, 43] or vertical melt transportation from weaker, smaller mantle upwelling cells [44].

The spacing of magmatically stronger segments on the Knipovich Ridge is 85–100 km, similar to segment spacing reported from the SWIR west of the Atlantis II FZ [45] where the mean axial depth is 4200 m. Along the Knipovich Ridge, the axial depth of the basement is deeper than the observed seafloor depth (mean = 3500 m) due to ~ 500 m

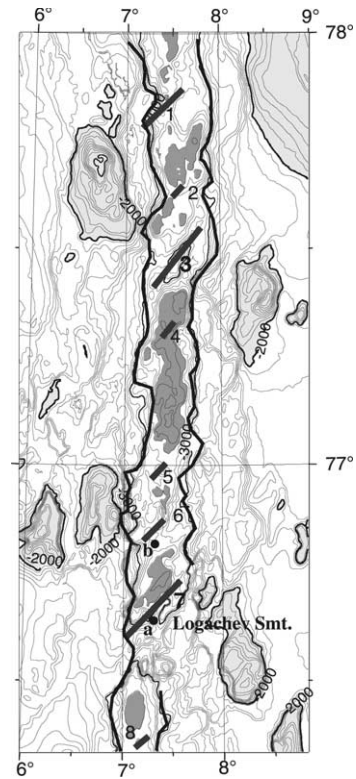


Fig. 5. Plan view of ridge segmentation pattern along the northern Knipovich Ridge. Bathymetry contour interval is 100 m and the basin deeper than 3500 m and the bathymetric highs greater than 2000 m are shown in dark and light gray, respectively. The rift wall (thick line) shows a zigzag pattern. Thick gray lines show the numbered ridge segments and solid black circles indicate the locations of sonar images shown in Fig. 4.

thick sediment [22,28]. Wider segment spacing is observed in the coldest portion of the SWIR east of Melville FZ where the mean depth is greater than 4500 m. The spacing between two large volcanic areas in the eastern Gakkel Ridge (full spreading rate is 10 mm/yr, mean axial depth is 4100 m) is also 110 km [8]. In the shallower slow spreading Mohns Ridge, the spacing of large MBA anomalies is 40–50 km [46]. Sauter et al. [45] suggested that the spacing of spreading cells is controlled by the viscosity and thickness of the convective layer in the SWIR, reflecting the large-scale thermal structure of the ridge system. Along the Arctic Ridges, wider segment spacing may also indicate cooler mantle beneath the ultraslow

spreading axes. The mean axial depth reflects the large-scale density structure, and the positive correlation between mean depth and segment spacing may indicate differences in mantle temperature among these ridges. Our comparison of ultraslow spreading systems is preliminary, because the resolution of our dataset is different from that of the SWIR. On- and off-axis high-resolution swath mapping and denser shipboard gravity measurement are required for more detailed consideration.

5.3. Effect of ridge obliquity

Three-dimensional modeling of the SWIR [47] indicates that the oblique portion of the ridge has a reduced effective spreading rate, slower mantle upwelling velocity, and lower temperature. However, the less oblique portion of the easternmost SWIR exhibits a deeper axis and lower volcanic production, suggesting cooler mantle in this area. Therefore, the effect of surface geometry, such as obliquity, seems to be a second-order factor compared to the large-scale thermal structure of the underlying mantle [44]. Along the Knipovich Ridge, the mean axial depth does not change over the ridge and the regional effect of the Iceland hotspot is negligible [48]. No transform faults or large offsets impose major along-axis changes in lithospheric thickness. These observations suggest that the large-scale thermal structure does not differ between the southern and northern sections of the ridge. In contrast, the obliquity changes abruptly from 35° north of 75°50'N to

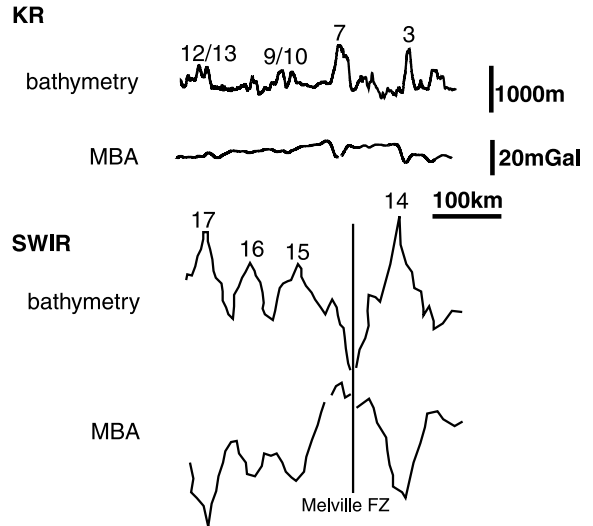


Fig. 6. Comparison of bathymetry and MBA profiles among the north and south Knipovich Ridge and Southwest Indian Ridge [34]. Segment numbers identified in this study (KR) and that of Cannat et al. [34] are shown. Key parameters are shown in Table 1.

49° south of that point. Therefore, comparing the northern and southern Knipovich Ridge is a reasonable test of the effect of obliquity on crustal accretion. A comparison of along-axis depths, MBA anomalies and other fundamental parameters of ultraslow spreading ridges (Fig. 6, Table 1) based on previous studies [8,34,46,49] shows that the scale of volcanic edifices tends to decrease as obliquity increases. High relief and large Δ MBA characterize the non-oblique segment of the SWIR, while low relief and small Δ MBA characterize the southern Knipovich Ridge (obliquity

Table 1
Comparison of segment characteristics among ultraslow spreading systems

	Ridge name		Mohns ^a	SWIR Seg 14 ^b	Seg 16 ^c	Seg 17 ^c
	Knipovich south	north				
Full spreading rate (mm/yr)	15	14	16	14	14	14
Relative plate motion direction (°)	306	307	300	0	0	1
General ridge trend (°)	347	002	058	066	055	090
Obliquity (°)	49	35	28	23	35	0
Bathymetric relief (m)	300	1000	~1000	2350	1300	2400
MBA minima (mGal)	< 10	20 ~ 25	< 15	40	16	38

^a Geli et al. [46].

^b Sauter et al. [49].

^c Cannat et al. [34].

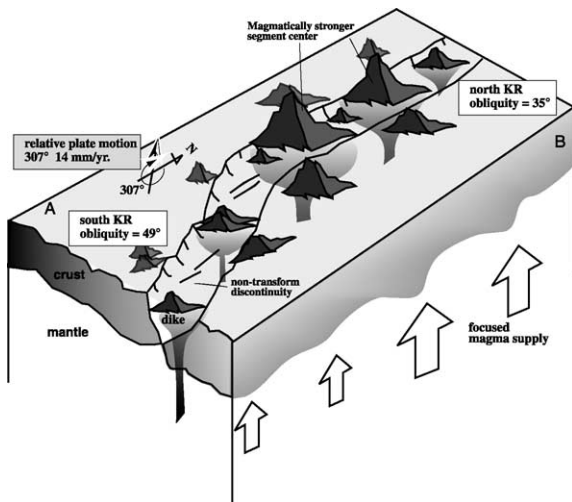


Fig. 7. Schematic illustrations for the contrast between the north and south Knipovich Ridge. Plane A is a plan view of the ridge and the along-axis section is projected to plane B. The axial valley is oblique to the spreading direction and the obliquity is much higher in the south. Large volcanic constructions that trend perpendicular to the spreading direction are located at the centers of the magmatically stronger segments, and the off-axis seamounts extend from these on-axis volcanic highs parallel to the spreading direction. The segment centers are lower and the deep non-transform discontinuities are more dominant along the southern Knipovich Ridge.

49°) and the oblique segment of the SWIR (obliquity 45°). This tendency is significant even if the sediment thickness on the Knipovich axial rift is taken into account. Sauter et al. [49] compared the normal and oblique segments in the SWIR and reported that the oblique section is associated with low Δ MBA and the areas of recent volcanism are distributed throughout low amplitude, elongated negative MBA areas, suggesting less focused accretion processes. Though the horizontal resolution of our analysis is lower and the coverage of the sonar image did not cover the entire rift width, the low relief with slight or no Δ MBA segments and the lava flows in the flat basins in the southern Knipovich Ridge indicate common characteristics between these highly oblique systems.

Discrete, focused magmatism is primarily controlled by the large-scale thermal structure of the mantle; however, rift geometry and kinematics also influence these processes. The southern Kni-

povich Ridge is characterized by low relief segment centers; these form due to high obliquity, low effective spreading rates, less adiabatic melting, and a resulting low melt supply. The dikes feeding the surface volcanoes intrude the oceanic crust perpendicular to plate motion; therefore, the horizontal extent of dikes is also limited in this highly oblique rift, resulting in smaller-scale bathymetric highs (Fig. 7). The estimated effects of ridge obliquity on upwelling velocity and on melt column thickness are a few percent, but these effects may be enhanced under colder mantle conditions [34]. Along the Knipovich Ridge, the effects of obliquity are enhanced by the slow spreading rates and the relatively colder mantle.

6. Summary

The results of our analysis and its implications for oblique, ultraslow spreading systems are summarized as follows and in Fig. 7.

1. The segmentation pattern of the Knipovich ridge is characterized by a few large volcanic constructions and deep, oblique non-transform discontinuities. This pattern is similar to that of the SWIR, another ultraslow, oblique spreading ridge with focused magma supply and localized volcanic activity at the ridge axis.
2. Two types of segments are defined. Magmatically stronger segments are more persistent and are spaced at intervals of 85–100 km, which may correspond to the spacing of mantle upwelling cells. These segments are accompanied by distinct MBA lows (northern part) or MBA perturbations (southern part), and off-axis traces of bathymetric highs.
3. Magmatically weaker segments have 300–500 m relief, slight or no MBA lows, and ambiguous off-axis traces. Most of them are located adjacent to magmatically stronger segments, sometimes separated by short non-transform discontinuities. The identification of these provisional segments may change when higher resolution data are collected; however, they are considered to be fed by lateral melt migration from adjacent segments or represent smaller, short-lived, discrete mantle upwelling centers.

4. Axial morphology changes clearly at 75°50'N, where the general trend of the axial valley changes from 000° in the north to 347° in the south. In the northern Knipovich Ridge, the volcanic constructions indicating focused magma supply exhibit higher relief (> 1000 m), in contrast to ~500 m relief in the southern area. Deep, flat basins are dominant in the south and the MBA varies only slightly.
5. Discrete, focused magmatism is primarily controlled by the large-scale thermal structure of the mantle; however, these processes are also influenced by shallower geometric and kinematic factors such as rift obliquity and plate separation rate. The contrast between the northern and southern Knipovich Ridge may indicate the effects of ridge obliquity on crustal accretion. Low-relief segment centers in the southern Knipovich Ridge may reflect high obliquity, low effective spreading rates, suppressed adiabatic melting, and resulting low melt supply.

Though the Knipovich Ridge is a good target area to understand the ultraslow spreading system and the effect of ridge obliquity, our analysis and the interpretation is limited, and preliminary because of poor data resolution especially in the southern part of the ridge. We would like to emphasize the necessity of a comprehensive field survey including the state-of-art multibeam bathymetry in the area.

Acknowledgements

We thank the officers and crew of the *R/V Prof. Logachev* for their assistance during the K2K cruise. We also thank G. Cherkasov, B. Baranov, E. Gusev and the Knipovich-2000 Scientific Party for their support and valuable discussion. Y. Nogi gave us kind advice about the satellite gravity in the arctic region. M. Coffin provided careful reviews. Critical comments from Y.J. Chen, D. Scheirer and two anonymous reviewers were very useful. Marine gravity data were supplied by S. Laxon, University College London and D. McAdoo, NOAA [26]. Figures were created using the public domain GMT software [50]./SK/

References

- [1] K.C. Macdonald, P.J. Fox, L.J. Perram, M.F. Eisen, R.M. Haymon, S.P. Miller, S.M. Carbotte, M.H. Cormier, A.N. Shor, A new view of the mid-ocean ridge from the behavior of ridge-axis discontinuities, *Nature* 335 (1988) 217–225.
- [2] E.M. Klein, C.H. Langmuir, Global correlations of ocean ridge basalt chemistry with axial depth and crustal thickness, *J. Geophys. Res.* 92 (1987) 8089–8115.
- [3] Y.J. Chen, Oceanic crustal thickness versus spreading rate, *Geophys. Res. Lett.* 19 (1992) 753–756.
- [4] J.W. Bown, R.S. White, Variation with spreading rate of oceanic crustal thickness and geochemistry, *Earth Planet. Sci. Lett.* 121 (1994) 435–449.
- [5] H.R. Jackson, I. Reid, R.K.H. Falconer, Crustal structure near the arctic mid-ocean ridge, *J. Geophys. Res.* 87 (1982) 1773–1783.
- [6] B.J. Coakley, J.R. Cochran, Gravity evidence of very thin crust at the Gakkel Ridge (Arctic Ocean), *Earth Planet. Sci. Lett.* 162 (1998) 81–95.
- [7] P.R. Vogt, P.T. Taylor, L.C. Kovacs, G.L. Johnson, Detailed aeromagnetic investigation of the Arctic Basin, *J. Geophys. Res.* 84 (1979) 1071–1089.
- [8] M.H. Edwards, G.J. Kurras, M. Tolstoy, D.R. Bohnenstiehl, B.J. Coakley, J.R. Cochran, Evidence of recent volcanic activity on the ultraslow-spreading Gakkel ridge, *Nature* 409 (2001) 808–812.
- [9] P. Michael, J. Thiede, H. Dick, S. Goldstein, D. Graham, W. Jokat, C. Langmuir, R. Muhe, J. Snow, Scientific Parties (Healy 0102 Polarstern ARK XVII/2), The Arctic Mid-Ocean Ridge expedition – AMORE 2001 – Seafloor spreading at the top of the world, *EOS Trans. AGU* 82, Fall Meet. Suppl. (2001) Abstr. T11B-0858.
- [10] V. Mendel, D. Sauter, L. Parson, J.R. Vanney, Segmentation and morphotectonic variations along a super slow-spreading center: the Southwest Indian Ridge (57°E–70°E), *Mar. Geophys. Res.* 19 (1997) 505–533.
- [11] L. Parson, D. Sauter, V. Mendel, P. Patriat, R. Searle, Evolution of the axial geometry of the Southwest Indian Ocean Ridge between the Melville Fracture Zone and the Indian Ocean Triple Junction – Implications for segmentation on very slow-spreading ridges, *Mar. Geophys. Res.* 19 (1997) 535–552.
- [12] C. Rommevaux-Jestin, C. Deplus, P. Patriat, Mantle Bouguer anomaly along an ultra slow-spreading ridge: implications for accretionary processes and comparison with results from central Mid-Atlantic Ridge, *Mar. Geophys. Res.* 19 (1997) 481–503.
- [13] J. Snow, H. Dick, A. Buechl, P. Michael, E. Hellebrand, Ship Sc. Parties HEALY102-POLARSTERN 59, Mantle partial melting beneath Gakkel Ridge reflected in the petrography of spinel lherzolites, *EOS Trans. AGU* 82, Fall Meet. Suppl. (2001) Abstr. T11B-0858.
- [14] K. Crane, A. Solheim, Seafloor Atlas of the Northern Norwegian-Greenland sea, Norsk Polarinstittut, Oslo, 1995.

- [15] P.R. Vogt, W.Y. Jung, J. Brozena, Arctic margin gravity highs: deeper meaning for sediment depocenters?, *Mar. Geophys. Res.* 20 (1998) 459–477.
- [16] K. Tamaki, G. Cherkashov, Knipovich-2000 Scientific Party, Japan-Russia cooperation at the Knipovich Ridge in the Arctic Sea, *InterRidge News* 10 (1) (2001) 48–51.
- [17] C. DeMets, R.G. Gordon, D.F. Argus, S. Stein, Current plate motion, *Geophys. J. Int.* 101 (1990) 425–478.
- [18] S.C. Cande, D.V. Kent, Revised calibration of the geomagnetic polarity timescale for the late Cretaceous and Cenozoic, *J. Geophys. Res.* 100 (1995) 6093–6095.
- [19] L. Geli, Volcano-tectonic events and sedimentation since Late Miocene times at the Mohns Ridge, near 72°N, in the Norwegian Greenland Sea, *Tectonophysics* 222 (1993) 417–444.
- [20] P.R. Vogt, L.C. Kovacs, C. Bernero, S.P. Srivastava, Asymmetric geophysical signatures in the Greenland-Norwegian and southern Labrador Seas and the Eurasia Basin, *Tectonophysics* 89 (1982) 95–160.
- [21] K. Crane, E. Sundvor, R. Buck, F. Martinez, Rifting in the Northern Norwegian-Greenland Sea: thermal test of asymmetric spreading, *J. Geophys. Res.* 96 (1991) 14529–14550.
- [22] E.A. Gusev, S.I. Shkarubo, The anomalous structure of Knipovich Ridge, *Russ. J. Earth Sci.* 3 (2) (2001) 145–161.
- [23] M. Abelson, A. Agnon, Mechanics of oblique spreading and ridge segmentation, *Earth Planet. Sci. Lett.* 148 (1997) 405–421.
- [24] M. Jakobsson, N.Z. Cherkis, J. Woodward, R. Macnab, B. Coakley, New grid of Arctic bathymetry aids scientists and mapmakers, *EOS Trans. AGU* 81 (2000) 89, 93, 96.
- [25] K. Crane, H. Doss, P. Vogt, E. Sundvor, G. Cherkashov, I. Poroshina, D. Joseph, The role of Spitsbergen shear zone in determining morphology, segmentation and evolution of the Knipovich Ridge, *Mar. Geophys. Res.* 22 (2001) 153–205.
- [26] S. Laxon, D. McAdoo, Satellites provide new insights into polar geophysics, *EOS* 79 (1998) 69, 72–73.
- [27] V.A. Childers, D.C. McAdoo, J. Brozena, S.W. Laxon, New gravity data in the Arctic Ocean: comparison of airborne and ERS gravity, *J. Geophys. Res.* 106 (2001) 8871–8886.
- [28] E. Sundvor, O. Eldholm, T.P. Gladchenko, S. Planke, Norwegian-Greenland sea thermal field, in: A. Nottvedt et al. (Eds.) *Dynamics of the Norwegian Margin*, Spec. Publ. 167, Geological Society, London, 2000, pp. 397–410.
- [29] B.Y. Kuo, D.W. Forsyth, Gravity anomalies of the ridge-transform system in the South Atlantic between 31 and 34.5°S: upwelling centers and variations in crustal thickness, *Mar. Geophys. Res.* 10 (1988) 205–232.
- [30] J. Lin, G.M. Purdy, H. Schouten, J.C. Sempere, C. Zervas, Evidence from gravity data for focused magmatic accretion along the Mid-Atlantic Ridge, *Nature* 344 (1990) 627–632.
- [31] O. Dauteuil, J.P. Brun, Oblique rifting in a slow-spreading ridge, *Nature* 361 (1993) 145–148.
- [32] O. Dauteuil, J.P. Brun, Deformation partitioning in a slow spreading ridge undergoing oblique extension: Mohns Ridge, Norwegian Sea, *Tectonics* 15 (1996) 870–884.
- [33] R. Thibaud, P. Genta, M. Maia, A systematic analysis of the Mid-Atlantic Ridge morphology and gravity between 15°N and 40°N: constraints of the thermal structure, *J. Geophys. Res.* 103 (1998) 24223–24243.
- [34] M. Cannat, C. Rommevaux-Jestin, D. Sauter, C. Deplus, V. Mendel, Formation of the axial relief at the very slow spreading Southwest Indian Ridge (49° to 69°E), *J. Geophys. Res.* 104 (1999) 22825–22843.
- [35] N.R. Grindlay, J. Madsen, C. Rommevaux, J. Sclater, A different pattern of ridge segmentation and mantle Bouguer gravity anomalies along the ultra-slow spreading Southwest Indian Ridge (15°30'E to 25°E), *Earth Planet. Sci. Lett.* 161 (1998) 243–253.
- [36] J.W. Head III, L. Wilson, D.K. Smith, Mid-ocean ridge eruptive vent morphology and substructure: evidence for dike widths, eruption rates, and evolution of eruptions and axial volcanic ridges, *J. Geophys. Res.* 101 (1996) 28265–28280.
- [37] K.C. Macdonald, D.S. Scheirer, S.M. Carbotte, Mid-ocean ridges: discontinuities, segments and giant cracks, *Science* 253 (1991) 986–994.
- [38] J.C. Sempere, J. Lin, H.S. Brown, H. Schouten, G.M. Purdy, Segmentation and morphotectonic variations along a slow-spreading center, the Mid-Atlantic (24°00'N–30°40'N), *Mar. Geophys. Res.* 15 (1993) 153–200.
- [39] Y. Niu, D. Bideau, R. Hekinian, R. Batiza, Mantle compositional control on the extent of mantle melting, crust production, gravity anomaly, ridge morphology, and ridge segmentation: a case study at the Mid-Atlantic Ridge 33–35°N, *Earth Planet. Sci. Lett.* 186 (2001) 383–399.
- [40] InterRidge, InterRidge Science Plan, <http://www.intridge.org/act1.html>.
- [41] D.K. Smith, J.R. Cann, The role of seamount volcanism in crustal construction at the Mid-Atlantic Ridge (24°–30°N), *J. Geophys. Res.* 97 (1992) 1645–1658.
- [42] L.S. Magde, D.W. Sparks, R.S. Detrick, The relationship between buoyant mantle flow, melt migration, and gravity bull's eyes at the Mid-Atlantic Ridge between 33°N and 35°N, *Earth Planet. Sci. Lett.* 148 (1997) 59–67.
- [43] L.S. Magde, A.H. Barclay, D.R. Toomey, R.S. Detrick, J.A. Collins, Crustal magma plumbing within a segment of the Mid-Atlantic Ridge, 35°N, *Earth Planet. Sci. Lett.* 175 (2000) 55–67.
- [44] J. PhippsMorgan, Y.J. Chen, The genesis of oceanic crust: magma injection, hydrothermal circulation and crustal flow, *J. Geophys. Res.* 98 (1993) 6283–6297.
- [45] D. Sauter, P. Patriat, C. Rommevaux-Jestin, M. Cannat, A. Briais, Gallieni Shipboard Scientific Party, the Southwest Indian Ridge between 49°15'E and 57°E: focused accretion and magma redistribution, *Earth Planet. Sci. Lett.* 192 (2001) 303–317.

- [46] L. Geli, V. Renard, C. Rommevaux, Ocean crust formation processes at very slow spreading centers: a model for the Mohs Ridge, near 72°N, based on magnetic, gravity, and seismic data, *J. Geophys. Res.* 99 (1994) 2995–3013.
- [47] J.E. Geogren, J. Lin, H.J.B. Dick, Evidence from gravity anomalies for interactions of the Marion and Bouvet hot-spots with the Southwest Indian Ridge: effects of transform offsets, *Earth Planet. Sci. Lett.* 187 (2001) 283–300.
- [48] J.-G. Schilling, R. Kingsley, D. Fontignie, R. Poreda, S. Xue, Dispersion of the Jan Mayen and Iceland mantle plumes in the Arctic, a He-Pb-Nd-Sr isotope tracer study of basalts from the Kolbeinsey, Mohs, Knipovich Ridges, *J. Geophys. Res.* 104 (1999) 10543–10570.
- [49] D. Sauter, L. Parson, V. Mendel, C. Rommevaux-Jestin, O. Gomez, A. Briais, C. Mevel, K. Tamaki, The FUJI scientific team, TOBI sidescan sonar imagery of the very slow-spreading Southwest Indian Ridge: evidence for along-axis magma distribution, *Earth Planet. Sci. Lett.* 199 (2002) 81–95.
- [50] P. Wessel, W.H.F. Smith, New version of the Generic Mapping Tools released, *EOS Trans. Am. Geophys. Union* 76 (1998) 329.